Regimes of precipitation change over Europe and the Mediterranean

Julie André[1,2], Fabio D'Andrea[1], Philippe Drobinski[1], Caroline Muller[3]

November 9, 2023

[1] Laboratoire de Météorologie Dynamique / Institut Pierre Simon Laplace, ENS - PSL Université, Ecole Polytechnique - Institut Polytechnique de Paris, Sorbonne Université, CNRS, France
[2] Ecole des Ponts, France
[3] Institute of Science and Technology Austria, Austria

Abstract

The Mediterranean region is experiencing pronounced aridification and in certain areas higher occurrence of intense precipitation. In this work, we analyze the evolution of the rainfall probability distribution in terms of precipitating days (or "wet-days") and all-days quantile trends, in Europe and the Mediterranean, using the ERA5 reanalysis. Looking at the form of wet-days quantile trends curves, we identify four regimes. Two are predominant: in most of Northern Europe the rainfall quantiles all intensify, while in the Mediterranean the low-medium quantiles are mostly decreasing as extremes intensify. The wet-days distribution is then modeled by a Weibull law with two parameters, whose changes capture the four regimes. Assessing the significance of the parameter changes over 1950–2020 shows that a signal on wet-days distribution has already emerged in Northern Europe (where the distribution shifts to more intense rainfall), but not yet in the Mediterranean, where the natural variability is stronger. We extend the results by describing the all-days distribution change as the wet-days', plus a contribution from the dry-days frequency change, and study their relative contribution. In Northern Europe, the wet-days distribution change is the dominant driver, and the contribution of dry-days frequency change can be neglected for wet-days percentiles above about 50%. In the Mediterranean, however, the contribution to all-days change of wet-days distribution change is much smaller than the one of dry-days frequency. Therefore, in the Mediterranean the increase of dry-days frequency is crucial for all-days trends, even when looking at heavy precipitations.

Key points :

- Four regimes of change for daily rainfall distribution are identified, and are captured by a two parameter analytical model.
- In Northern Europe, a signal of increasing mean and extreme precipitations has emerged.
- In the Mediterranean, the changes of rainfall appears dominated by changes in dry-days frequency.

1 Introduction

Climate change is known to impact the global water cycle, and to have consequences on total rainfall and extreme of precipitations. The changes expected on total precipitations are of about +2-3% per degree Celsius of global warming, while for the extreme rainfalls, estimates from thermodynamics give at first order a rise in intensity of about 7%/°C (Trenberth, 1999; Allen and Ingram, 2002; Held and Soden, 2006). However, on regional scales the changes in mean and extreme precipitation can vary substantially from the global mean, due both to dynamical aspects and natural variability (Trenberth, 2011; Fischer et al., 2013; Pendergrass and Hartmann, 2014; Fischer and Knutti, 2014; Pfahl et al., 2017).

The Mediterranean region, due to its unique position as a transition zone between the wetter Europe and the dryer desert of the Sahara, is a climate change hotspot in terms of temperature and precipitation changes (Giorgi, 2006). Climate simulations predict that the Mediterranean will get drier (more evaporation and decreased mean precipitation) with global warming (D'Agostino and Lionello, 2020; Drobinski et al., 2020) and will experience more extreme rainfalls, at least on the northern shore (Vautard et al., 2014; Giorgi et al., 2014; Drobinski et al., 2018; Myhre et al., 2019; Pichelli et al., 2021; Ali et al., 2022).

This simultaneous decrease in mean precipitations and increase in extreme rainfalls is sometimes called a "paradox in the water cycle change" (Brunetti et al., 2000; Alpert et al., 2002; Brunetti, 2004). Northern Western and Central Europe, on the contrary, are expected to undergo an increase of both total precipitations and extreme rainfalls (Intergovernmental Panel On Climate Change, 2023, chapter 8).

Still, the long-term water cycle changes on the Mediterranean are unclear when looking at historical observations. In observations, previous studies find a strong and significant signature of increasing evaporation and of drier conditions, such as droughts or dry spells (Hoerling et al., 2012; Sheffield and Wood, 2012; Raymond et al., 2016; Caloiero et al., 2018), associated to an increase of dry-days frequency over the Mediterranean and an increase over Europe (Brunetti et al., 2000; Brunetti, 2004; Benestad et al., 2019), but the trends of the mean precipitations are subject to more debate. The 6th IPCC assessment report (Intergovernmental Panel On Climate Change, 2023, chapter 8) concludes that there is no long-term trend of the mean precipitation in the Mediterranean since the pre-industrial era. Only on shorter time periods of the order of a few decades or on sub-regions can some significant trends be derived (Sousa et al., 2011; Tanarhte et al., 2012; Mariotti et al., 2015; Zittis, 2018), but they may be driven mainly by natural variability and not by climate change (Peña-Angulo et al., 2020).

In this paper, we want to study the whole rain distribution over the Mediterranean region. Compared to droughts and extreme precipitations which have been extensively studied, the research on the whole rain distribution is relatively less developed. In the few papers that do study the whole range of the rain distribution, two main approaches can be distinguished: non-parametric and parametric studies. Non-parametric studies focus on the changes of frequency of fixed rain intensity amounts or on the changes of intensity for fixed percentile rank or on the change of contribution from given rain amounts to the total precipitation (Alpert et al., 2002; Brunetti, 2004; Klingaman et al., 2017; Berthou et al., 2019, 2020). These methods are interesting, but when one wants to allow diagnostics or interpretation in terms of a few key parameters, parametric studies are needed.

Still, very few parametric studies do not focus only on the extreme precipitations. Some of them have taken a simple exponential law (Benestad et al., 2019) or a gamma law which performs quite well for the low to medium precipitations (Ben-Gai et al., 1998; Groisman et al., 1999), or a Generalized Pareto Distribution from generalized extreme values theory, which is known to be suited for high amounts but not necessarily for the medium amounts. A more complex model, tailored for wet-days precipitation, has been recently proposed by Naveau et al. (2016) and gives very good results for both the low rainfall and the extremes (Tencaliec et al., 2020; Rivoire et al., 2022), still with a little more complexity (it has three parameters compared to two for the gamma law or one for the exponential). In this paper, we choose the intermediate approach of a Weibull law with two parameters, which, as will be shown below, represents a minimal framework to model wet-days distribution and its quantile trends regimes.

In this work, we propose a framework which describes the change over time of the whole distribution of precipitation: from absence of rain to low and moderate rainfall, up to extreme events. We first perform a description of the wet-days trends, quantile by quantile. As underlined by Schär et al. (2016), such a method should consider the change in frequency of precipitating days (or "wet-days"). Therefore, we also study how the wet-days quantile trends can be influenced by the change in dry-days frequency. We illustrate this methodological framework on the recent past in Europe and the Mediterranean. The main question addressed here is the following: how does the whole precipitation distribution change across Europe and the Mediterranean region?

The outline of the paper is as follows: Section 2 presents the dataset used, then Section 3 presents the different kinds of regimes that can be observed over Europe and the Mediterranean concerning the wet-days quantile trends. Section 4 proposes the Weibull law as a wet-days distribution to represent the observed regimes, and analyze them more thoroughly. Section 5 extends this parametric model to the all-days distribution, with an application on the trends of the total precipitation and of all-days quantiles.

2 Precipitation dataset

The choice of the data set was driven by the need for a homogeneous data over the Mediterranean region, as well as long-term time series to help detect small changes in the precipitation distribution.

We choose not to use EOBS gridded data, although it is considered as the reference of its kind for Europe and covers a long enough period (since 1950) at 0.25° resolution, because it suffers temporal and spatial inconsistencies (Cornes et al., 2018). Indeed, EOBS rainfall dataset is based on the spatial interpolation of rain gauge data from stations which number and density have changed significantly over time, therefore one is advised not to use it for the analysis of long-term trends.

Since most of the over available observational data sets cover either a smaller domain (IBERIA01 in Portugal and Spain (Herrera et al., 2019), or CARPATCLIM covering the Carpathians), a shorter period of time (the IMERG reanalysis product starts in 2000, the FROGS product in the 1970s), or have a coarser temporal or spatial resolution (CRU starts is a monthly dataset, while REGEN is daily but at 1°), we turned to ERA5 reanalysis.

We used ERA5, the latest global reanalysis provided by the European Center for Medium-Range Weather Forecasts (Hersbach et al., 2020), at a resolution of 0.25°, on the period 1950-2020. We computed the daily accumulated rainfall from ERA5 hourly variable "total precipitation", which incorporates both convective and large-scale precipitation.

Note that if microwave radiances and ground radar rain rates are assimilated in ERA5, rain gauges data are not assimilated for the rainfall product. Rivoire et al. (2021) showed that ERA5 tends to overestimate precipitation occurrence (for 1 mm/day threshold) over European lands by about 10 to 20% compared to EOBS gridded data set, and even more over sea surface (when compared with CMORPH global data set). Therefore, we must keep in mind ERA5 general bias on precipitations. Still, ERA5 precipitation wet-days intensity has been shown to be in very good agreement with EOBS gridded data set over European lands, where the station density is high (especially Germany, Ireland, Sweden, and Finland), and over the mid-latitude seas, compared with CMORPH.

Our domain covers the area between 25°W and 45°E in longitude, and between 25°N and 71°N in latitude, enabling the study of both the Mediterranean and Europe.

Finally, we would like to highlight that the methodology we present in this paper can be applied to any other rainfall data sets.

3 Observed regimes for the change of the wet-days distribution

One way to study the distribution changes of precipitation is to look at the cumulative density function (CDF) or equivalently at the quantile curve (i.e., the inverse of the CDF). To see their evolution with time, we can choose two periods of time, subtract their quantile curves, and obtain the curve of the intensities of the quantile trends for all percentiles. In the following, we designate as trend the absolute change of a given variable between two periods of 31 years, 1950–1980 and 1990–2020, divided by the time interval between the two periods, four decades here. We choose to take periods of three decades to smooth out the natural variability within those periods when taking the mean statistics. The impact on our results of the choice of the dates is negligible (see Section 7.1).

A rainfall distribution usually has a high probability of the event 0 mm, corresponding to the many dry-days, i.e. days with no to low rainfall accumulation. In this paper, we will look at both the change of rainfall occurrence and intensity of rain (i.e. wet-days distribution) but also the all-days distribution. For methodological issues, it is indeed handy to set aside the dry-days and fit a model on the wet-days distribution only (which will be done in the next section). We are conscious that a quantile trend defined on a wet-days distribution may be influenced by a change in the fraction of dry-days, f_d, as discussed in detail in Schär et al. (2016): this aspect will be further developed in the next section.

The work from Expert Team on Climate Change Detection and Indices recommends the use of 1 mm/-day as the threshold for the definition of dry and wet-days: this value enables to better deal with both the issues of under-reporting of small rainfall amounts in observations and the "drizzle problem" of models and reanalyses - which usually have too many days with weak rain (Karl et al., 1999; Zhang et al., 2011). The fraction of dry-days (less than 1 mm/day) is far from being negligible in our domain, and can vary from 20% in Northern Europe up to 90% in the Maghreb (and almost 100% in the desert). Note that by construction, the trend of the 0% wet-days percentile will always be zero, as its intensity is by definition fixed to 1 mm/day.

Figure 1 illustrates four main qualitatively different shapes that can be found on the domain. They depend on the evolution of the CDF :

- all quantiles increasing (for ex. in the UK),
- all quantiles decreasing (for ex. in the North of Portugal),
- a U-shape regime, consisting in negative trends for low to medium quantiles but positive trends on extremes, with a certain inversion percentile in between (for ex. in the North of Italy),
- a reversed U-shape regime, with increasing low to medium percentiles with decreasing extremes (for ex. in the Mediterranean Sea, North of Libyan coast).

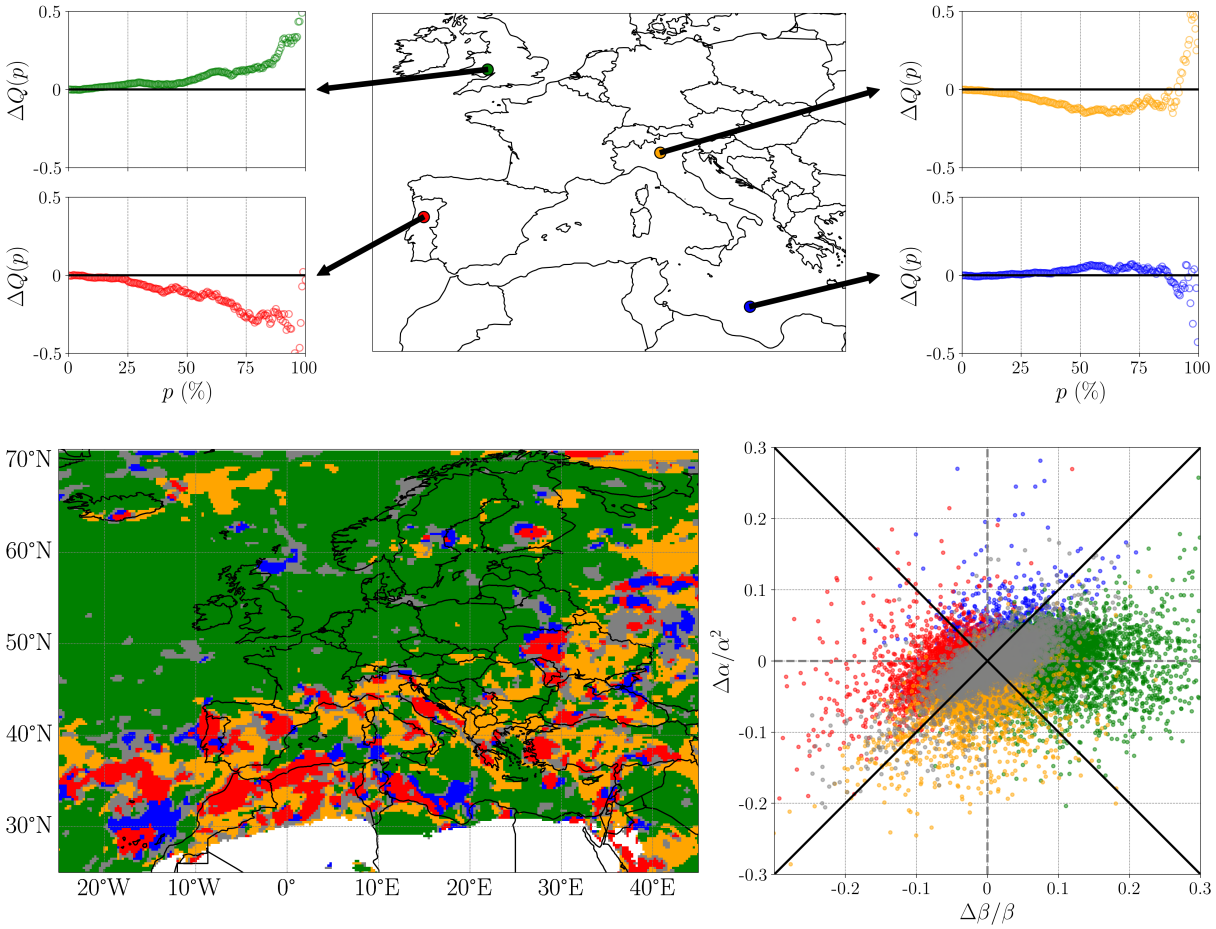

Figure 1: Top: illustration of the four types of behaviors for wet-days quantile trend curve (between 1950–1980 and 1990–2020), at four chosen locations. The quantile trends $\Delta Q(p)$ are plotted in mm/-day/decades. Bottom left: category map obtained from the classification algorithm, applied on the trends between 1950–1980 and 1990–2020, with a sliding window of 9 grid-points. Green corresponds to "all quantiles intensify" category, red to "all quantiles decrease", orange to "U-shape" and blue to "reverse U-shape". Gray means the category is unclear. White designates desert location (less than 2% of wet-days). Bottom right: relative change of Weibull parameters $\left(\frac{\Delta\beta}{\beta}, \frac{\Delta\alpha}{\alpha^2}\right)$ for the whole domain. Colors indicate as before the category detected by the classification algorithm. The black thick lines are the theoretic limits between the influence zones of the two Weibull parameters.

Note that a regime comparable to this "U-shape", with an "inversion percentile" or "crossover", was already mentioned in literature for the Mediterranean region (Boberg et al., 2010; Colin, 2011).

In order to quantitatively distinguish between those regimes of trends, we developed a simple classification algorithm, which takes in input a list of percentiles and associated quantile trends, looks at the shape of the trend curve and assesses in which of the four categories it falls into. It uses both the signs of the trends and of the trends slope, for low to medium ranks as well as for extreme high ranks. The full definition of the algorithm is in Section 7.1.

This classification algorithm was applied over the whole Mediterranean and European domain, between 1950–1980 and 1990–2020, giving the category map shown in Figure 1. We added a category "unknown" (in gray) for the points whose category was unclear. Note that this map was obtained by applying the algorithm on a sliding window of 9 pixels (which for each grid-point merges together the time series of its 8 neighboring grid-points) to smooth out very local irregularities.

The first thing that becomes manifest on the category map in Figure 1 is a clear North/South pattern: a large majority of North-West Europe as well as subtropical Atlantic Ocean belongs to the same category ("all rain quantiles intensify"), while the Mediterranean region is mainly in the "U-shape" category (i.e., decreasing low to medium quantiles but increasing extremes) with also a certain amount of "all rain quantiles decrease" category. This is consistent with what one would expect from a Mediterranean type behavior, with both drying and extreme rain events intensification. In the southern part of the Mediterranean basin, the "all decrease" regime is more predominant. We remind that the differences between the "all-decrease" and "U-shape" categories are mainly due to their opposite trend signs for very heavy precipitations. We can also observe that for the Mediterranean Sea waters far from the land coasts (about 200 km away), the dominant category is the "all rain quantiles intensify" one. As for African land equatorward of 30°N, the category map becomes extremely spotty, which could be due to a higher natural variability in the wet-days distribution, mainly due to the very small number of wet-days. Therefore, we won't look at desert regions, where there is less than 2% of rainy days.

We also note that the map of categories is much spottier within the Mediterranean region than in Northern Europe. This spottiness seems to be mainly due to a strong natural variability, from which a long-term climate change signal in the Mediterranean on the wet-day distribution has not yet emerged. Indeed, as shown in Section 7.1, the agreement between wet-days category maps computed for different time periods (of 20 to 35 years) is much lower for the Mediterranean than Northern Europe. The spottiness of the category map in the Mediterranean is probably an illustration of the sampling error.

As a sum up, the signal of an intensification in the wet-day distribution is clear in Northern Europe, while the Mediterranean region does not seem to have a strong signal yet, at least not strong enough to overcome the noise of natural variability. This is a motivation to try to improve the significance of a signal by taking a parametric approach.

4 Analytical model for the wet-days rain distribution

In order to synthesize the information on each and every quantile trends into a smaller number of parameters, we turn to a parametric approach.

We first focus on finding a model for the wet-days distribution. Then in Section 5 we will see how all-days quantiles trends can be influenced by the changes of both the wet-days distribution and the dry-days frequency.

Benestad et al. (2019) used an exponential law for the wet-days rain distribution, which works well on the observational data and gives a good "rule of thumbs" to relate extremes probability or quantile trends to the wet-days mean. However, since this wet-days model has a single parameter (the wet-days mean), this model can only represent a shift of all quantiles to higher (resp. lower) intensities if the parameter increase (resp. decrease). Thus it can not represent the two other quantile trends behaviors we observe, the "U-shape" and "reversed U-shape", which have an opposite trend for low and high percentile. We need at least two parameters in the wet-days distribution in order to represent the four observed regimes.

We compared different models having two or three parameters, among usually-used models for rain distribution (Gamma, Weibull, Lognormal, Pearson, etc.) on our precipitation dataset, using the maximum likelihood estimation method. We used Kolmogorov-Smirnov and Cramer von Mises metrics as goodness of fit estimators. More details about the fit, the comparison of the different models and the adjustment tests are given in Section 7.1. The comparison indicates that a Weibull model with two parameters is a good option for ERA5 wet-days distribution, with only a small number of parameters.

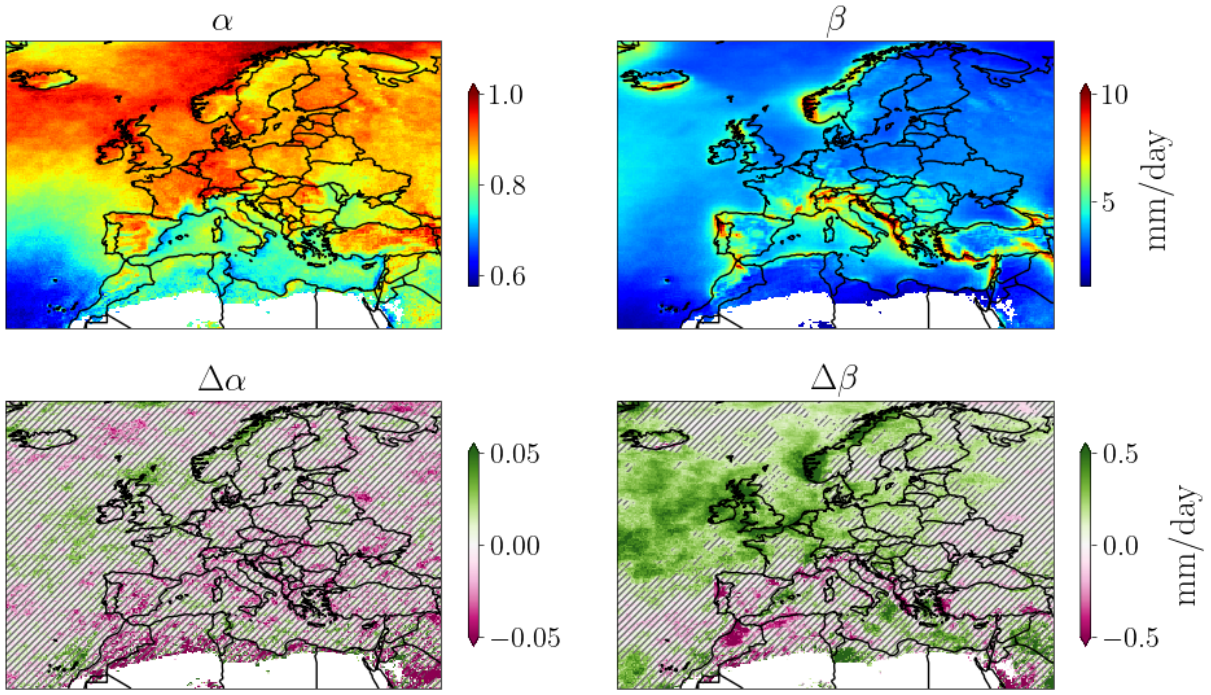

Figure 2: Results for the Weibull parameters fitted on ERA5 wet-days rain distribution. Top row: Weibull shape parameter α and scale parameter β on the period 1950–1980. Bottom row: absolute changes between 1950–1980 and 1990–2020. The hatches denote the location where the change is not significant through a bootstrap test, at a confidence level of 90%.

A Weibull distribution is defined by two parameters: a shape parameter (called α) and a scale parameter (called β). The cumulative density function of a Weibull law is expressed as:

$$g(x) = 1 - e^{-(x/\beta)^{\alpha}}$$

where x is the intensity of rainfall, and $p = g(x) \in [0, 1]$ is the probability to have a wet-days with a rainfall inferior to x. Note that p is also the percentile rank corresponding to an event of intensity x. Note that α and β are both positive, and $\alpha \leq 1$. β can be thought of as representative of the distribution median and has a unit of mm/day, while α is linked to the variance but is dimensionless. For a given percentile p, the quantile intensity $Q(p)$ in mm/day is obtained as the inverse of the cumulative density function:

$$Q(p) = x = \beta \left[\ln \left(\frac{1}{1-p} \right) \right]^{1/\alpha} \tag{1}$$

In Equation (1) it becomes clear that β is the quantile of rank $p = 1 - e^{-1}$, thus $\beta \approx Q(63\%)$ and we can think of β as quite close to the wet-days rain median. When $\alpha \to 1$, the Weibull model simplifies to an exponential distribution, giving the same expressions as in Benestad et al. (2019), with the parameter β becoming the wet-days mean.

Quantile trend curves like the ones shown in Figure 1 can be expressed analytically as $\Delta Q(p)$, Δ denoting the change between two periods of time:

$$\Delta Q(p) = Q_2(p) - Q_1(p) = \beta_2 \left[\ln \left(\frac{1}{1-p} \right) \right]^{1/\alpha_2} - \beta_1 \left[\ln \left(\frac{1}{1-p} \right) \right]^{1/\alpha_1} \tag{2}$$

using the subscripts 1 and 2 to denote two periods of time. This expression is simple and depends on only four parameters: $(\alpha_1, \beta_1, \alpha_2, \beta_2)$, or equivalently $(\alpha_1, \beta_1, \Delta\alpha, \Delta\beta)$. The values of those parameters for ERA5 rain data are displayed on Figure 2, along with the statistical significance of the changes (computed by a bootstrap test, as explained in Section 7.1).

We observed (not shown here) that a change in the scale parameter β, keeping α fixed, gives the category "all rain quantiles intensify" (for $\Delta\beta > 0$) or "all rain quantiles decrease" (for $\Delta\beta < 0$). In opposition, a change in the shape parameter α keeping β fixed gives either a U-shape (for $\Delta\alpha < 0$) or a

reversed U-shape category (for $\Delta\alpha > 0$). Note that when β, which is the quantile of rank approximately 63%, is constant, then the percentile of inversion is fixed at this precise rank: $p_{inv} = 63\%$.

When both parameters change at the same time, their two effects will add up, with a weight depending on the relative change of α and β. Considering small relative changes, i.e. $\frac{\Delta\alpha}{\alpha} \ll 1$ and $\frac{\Delta\beta}{\beta} \ll 1$, the quantile trends for a Weibull law can be written, at the first order, as:

$$\forall p \in (0,1),\ \Delta Q(p) \approx \frac{\partial Q}{\partial \alpha}(p)\ \Delta\alpha + \frac{\partial Q}{\partial \beta}(p)\ \Delta\beta \tag{3}$$

with the following expressions for the partial derivatives:

$$\frac{\partial Q}{\partial \alpha}(p) = -\frac{\beta}{\alpha^2} \ln\left(\ln\frac{1}{1-p}\right)\left(\ln\frac{1}{1-p}\right)^{1/\alpha}$$
$$\frac{\partial Q}{\partial \beta}(p) = \left(\ln\frac{1}{1-p}\right)^{1/\alpha}$$

The sensitivity of the trend curve to the two parameters α and β can be expressed as a simple ratio:

$$\left|\frac{\frac{\partial Q}{\partial \alpha}(p)\Delta\alpha}{\frac{\partial Q}{\partial \beta}(p)\Delta\beta}\right| = \frac{\beta}{\alpha^2}\left|\frac{\Delta\alpha}{\Delta\beta}\right|\left|\ln\left(\ln\frac{1}{1-p}\right)\right| \tag{4}$$

The change in α dominates the trend curve if it dominates the trends of at least the low percentiles and the tail. When plotting the logarithmic term with regard to the percentile p, we realize that this term has magnitude of order unity (except in the very near vicinity of $p = 0, 1-e^{-1}, 1$). Thus, we will take the approximation that the logarithmic term is of order unity on the ranks that are of interest for distinguishing between the different regimes. Finally, we come to the following result: the change in α dominates over β in the trend curve when:

$$\left|\frac{\Delta\alpha}{\alpha^2}\right| \gg \left|\frac{\Delta\beta}{\beta}\right| \tag{5}$$

i.e. knowing which of the change of the parameter α or β dominates the trend curve boils down to comparing their normalized changes. Therefore, in the space $\left(\frac{\Delta\beta}{\beta}, \frac{\Delta\alpha}{\alpha^2}\right)$, the two diagonals ($\left|\frac{\Delta\beta}{\beta}\right| = \left|\frac{\Delta\alpha}{\alpha^2}\right|$) theoretically set the approximate limits between the four rain quantile trend regimes:

- a U-shape for $\left|\frac{\Delta\beta}{\beta}\right| \ll \left|\frac{\Delta\alpha}{\alpha^2}\right|$ and $\Delta\alpha < 0$
- a reversed U-shape for $\left|\frac{\Delta\beta}{\beta}\right| \ll \left|\frac{\Delta\alpha}{\alpha^2}\right|$ and $\Delta\alpha > 0$
- all quantiles intensify for $\left|\frac{\Delta\beta}{\beta}\right| \gg \left|\frac{\Delta\alpha}{\alpha^2}\right|$ and $\Delta\beta > 0$
- all quantiles decrease for $\left|\frac{\Delta\beta}{\beta}\right| \gg \left|\frac{\Delta\alpha}{\alpha^2}\right|$ and $\Delta\beta < 0$

We can compare these theoretical limits with the four categories obtained by the detection algorithm (which makes no assumption on a distribution model). In Figure 1, we plotted all grid-points of the domain in the normalized Weibull phase space, and colored them by their category as detected by the classification algorithm. We see that indeed, the bottom part of the plot is mainly occupied by "U-shape" gridpoints (orange), the left part mainly "all decrease" category (red) and the right part mainly "All quantiles intensify" (green) points. Thus, the Weibull analytical limits are in very good agreement with the empirical categories.

On this figure, we can furthermore get an estimation of the rank of the inversion percentile p_{inv}, when it exists, from the angle a point makes in this normalized Weibull phase space. As explained in more details in Section 7.1, we have a direct link between the wet-days inversion percentile and the normalized changes of α and β, at first order:

$$p_{inv} \approx 1 - \exp\left(-\exp(\frac{\Delta\beta}{\beta}\frac{\alpha^2}{\Delta\alpha})\right). \tag{6}$$

In summary, we have used a Weibull model on the wet-days rainfall distribution to reduce the information of the quantile trend curve to two parameters and their change $(\alpha, \beta, \Delta\alpha, \Delta\beta)$. These parameters are enough to separate between the four observed wet-days regimes, and even to estimate the percentile of inversion p_{inv} when it exists.

5 Influence of the changes of both the wet-days distribution and dry-days frequency

5.1 Impact on annual mean

In order to illustrate the importance of taking into account not only the wet-days distribution but also the change of the dry-days frequency, we study their relative contributions to the all-days mean precipitation (i.e., total annual precipitation), which is one of the most studied parameters in climate change studies.

The all-days mean $\bar{x}$ is the mean of the daily rainfall intensity, and can be equivalently computed as the product of the wet-days frequency $f_w = 1 - f_d$ with the wet-days precipitation mean μ:

$$\bar{x} = (1 - f_d)\ \mu$$

The change of the all-days mean is due both to the change of dry-days frequency $f_d = 1 - f_w$ and to the change of wet-days mean:

$$\frac{\Delta\bar{x}}{\bar{x}} = -\frac{\Delta f_d}{(1 - f_d)} + \frac{\Delta\mu}{\mu} \tag{7}$$

Those two terms can either be of the same sign and add up to each other, or be of opposite signs and tend to cancel each other out. Indeed, there could be more wet-days but with less intense rain, which could result in an almost zero trend on the mean precipitation. Conversely, there could be regions with fewer wet-days but higher rain intensity when it rains, as was shown in future projection by Pierce et al. (2013) for California and by Polade et al. (2014) for Mediterranean type climates. The relative weight of the two terms is also important to study. For future projection, Polade et al. (2014) showed that the change in the occurrence term will dominate the change in intensity for the all-days mean, in most of the subtropics. However, there is very little literature on the behavior of these two terms in past data.

For a Weibull distribution, we can further detail the dependency of the wet-days mean on the shape and scale parameters. The expression of the Weibull mean is $\mu = \beta\ \Gamma\,(1 + 1/\alpha)$, where Γ denotes the Gamma function. Taking the logarithmic derivative of the mean, and using the definition of the Digamma function (usually noted ψ) as the derivative of the log of the Gamma function, we get:

$$\frac{\Delta\mu}{\mu} \approx \frac{\Delta\beta}{\beta} - \frac{\Delta\alpha}{\alpha^2}\left(\frac{d\ln\Gamma}{dz}\right)_{z=1+1/\alpha} = \frac{\Delta\beta}{\beta} - \frac{\Delta\alpha}{\alpha^2}\psi(1 + 1/\alpha) \tag{8}$$

Note that the Digamma function is strictly positive for the typical range of the shape parameter for ERA5 precipitation, thus the sign of the shape parameter contribution is given by $-\Delta\alpha$. Its typical values are $\psi(1 + 1/\alpha) \in [0.4, 1]$ for $\alpha \in [0.5, 1]$ which is the typical range for Europe and the Mediterranean. Thus, even in regions with a U-shape categories, where $\Delta\alpha$ dominates the wet-days trend curve as $\frac{|\Delta\beta|}{\beta} < \frac{|\Delta\alpha|}{\alpha^2}$, the change in wet-days mean is not necessarily dominated by $\Delta\alpha$, since the Digamma factor is smaller than 1.

Finally, we conclude that the relative change of the all-days mean can be decomposed in three contributions, from the relative changes of f_d, α and β:

$$\frac{\Delta\bar{x}}{\bar{x}} \approx -\frac{\Delta f_d}{(1 - f_d)} + \frac{\Delta\beta}{\beta} - \frac{\Delta\alpha}{\alpha^2}\ \psi(1 + 1/\alpha) \tag{9}$$

Figure 3 shows the relative contributions of those terms to the all-days mean. For Northern Europe, the two terms are of the same sign (decrease of dry-days frequency and more intense rainfall in average), but the all-days mean change is mainly due to the increase of the wet-days mean (the latter being mainly due to the increase of the Weibull scale parameter β). In a central European band between East France and Poland, the change of occurrence is close to zero, and the change in wet-days mean is the sole contributor to the all-days mean. For the Mediterranean region on the contrary, the two terms can have the same or opposite signs, but the increase of dry-days frequency is largely dominant, leading to a decrease of all-days mean.

Both in Northern Europe and in the Mediterranean (even in U-shape regions), the changes of the wet-days mean are mainly due to the scale parameter β, while the term due to the change of the scale parameter α is smaller in intensity.

We can check how well this first order approximation and Weibull model enable to capture the change in all-days means. We compare in Figure 4 the all-days mean (computed directly from data) to the sum

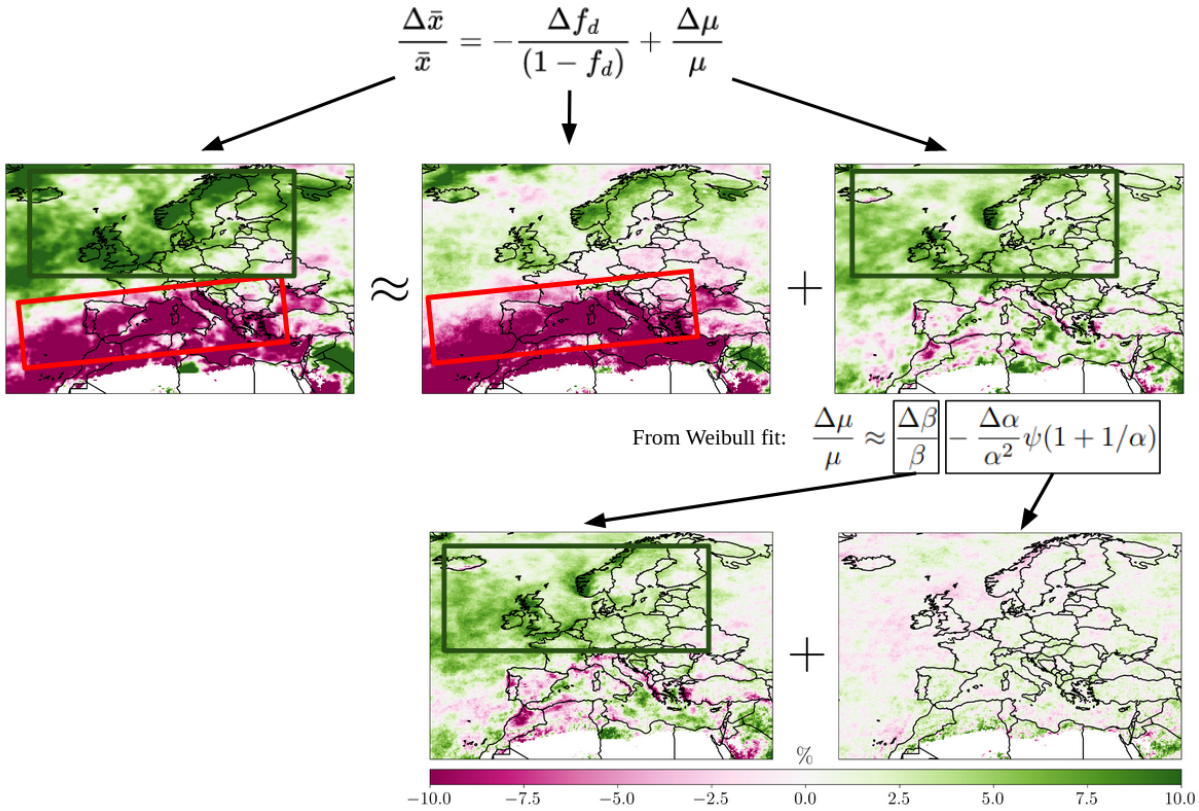

Figure 3: The different contributions to the all-days mean change, between 1950–1980 and 1990–2020, from the dry days frequency and the wet-days mean, the latter decomposed into contributions from its two parameters. Every map has the same scale for the color-map (given at the bottom of the figure). The green and red boxes highlight the difference between Northern Europe and the Mediterranean.

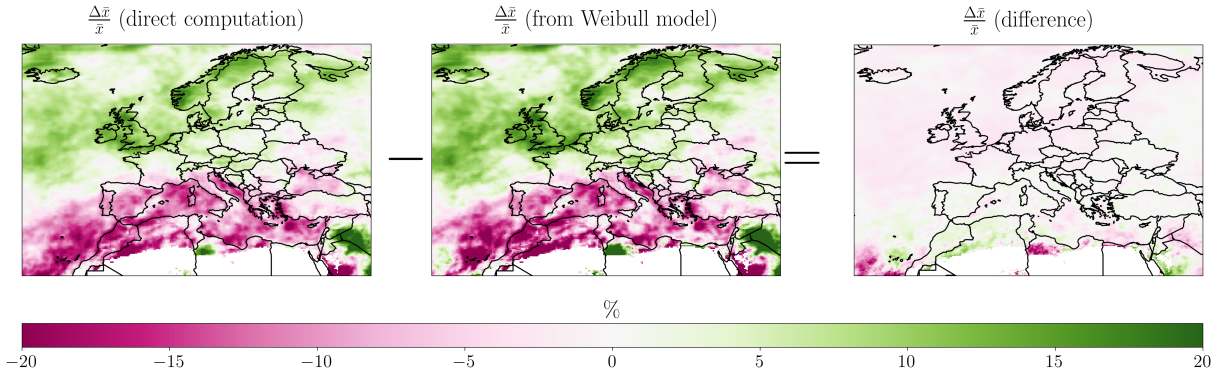

Figure 4: Relative change of all-days mean $\frac{\Delta\bar{x}}{\bar{x}}$, between 1950–1980 and 1990–2020, computed directly on data, compared to estimated from the Weibull model, i.e the three contributions from f_d, α and β.

of the f_d, α and β terms in Equation (9). This figure shows that the Weibull model for the intensity plus the rainfall occurrence capture most of the features of the all-days mean. Except for the lower latitudes where the error can reach 10%, the difference between the direct computation and the sum term is indeed only of a few percent, in Europe and the Mediterranean.

5.2 Influence on all-days quantiles trends of the dry-days frequency

In this section, we investigate in more detail the link between all- and wet-days precipitation quantiles. In order to understand and quantify how looking at wet-days only can impact the values of the trends for all-days quantiles, we follow the framework proposed by Schär et al. (2016), more precisely the derivation made in their first appendix.

The all-days rainfall distribution is linked to the wet-days' one by the dry-days frequency f_d. More precisely, the wet-days percentile p, which denotes the probability of having an event of intensity smaller or equal than x mm/day, and the all-days percentile p_a for the same rainfall intensity, are linearly linked by f_d :

$$p_a = (1 - f_d)p + f_d \tag{10}$$

Note that this formula is valid for any percentile rank as far as $p_a \geq f_d$. It gives indeed that for $p = 0$ we have $p_a = f_d$ and that the probability of the maximum rain value is the same ($p = 1$ when $p_a = 1$). This simple formula shows that a wet-days percentile p is linearly linked to the all-days percentiles p_a.

By definition, the wet-days quantile Q is equal to the all-days quantile Q_a for percentiles where they are both defined:

$$\forall p_a \in [f_d, 1], Q(p) = Q_a(p_a) \tag{11}$$

We now consider a change between periods 1 and 2 of the wet-days rain distribution and its quantiles Q: $\Delta Q = Q_2 - Q_1$, where Δ denotes again the change. For a fixed wet-days percentile p, ΔQ is related to the change of the all-days rank and quantile intensity, but also to the change in dry-days frequency. Rewriting with our notations the equation A7 from the appendix of Schär et al. (2016) gives:

$$\Delta Q(p) = \Delta Q_a(p_a) + \frac{\Delta f_d}{1 - f_d}(1 - p_a)\frac{\partial Q_{a,2}}{\partial p_a} \tag{12}$$

We would like to express analytically the slope of the quantile curve $\frac{\partial Q_{a,2}}{\partial p}$, with the Weibull model developed earlier. Thus, we come back to the slope of the wet-days quantiles, by using Equation (11) and the chain rule:

$$\frac{\partial Q_{a,2}(p_a)}{\partial p_a} = \frac{\partial Q_2(p)}{\partial p_a} = \frac{\partial Q_2(p)}{\partial p}\frac{\partial p}{\partial p_a}$$

Since the percentiles p and p_a are linearly linked, $\frac{\partial p}{\partial p_a} = \frac{1}{1-f_d} = \frac{1-p}{1-p_a}$, we get the following relationship between the two quantiles slopes:

$$(1 - p_a)\frac{\partial Q_{a,2}}{\partial p_a} = (1 - p)\frac{\partial Q_2}{\partial p}$$

Thus, Equation (12) becomes:

$$\Delta Q(p) = \Delta Q_a(p_a) + \frac{\Delta f_d}{1 - f_d}\,(1 - p)\frac{\partial Q_2}{\partial p} \tag{13}$$

Finally, we can apply the general formula in Equation (13) to a Weibull distribution of shape parameter α and scale parameter β. Putting all the terms depending on the wet-days percentile p on the same side, it yields:

$$\Delta Q_a(p_a) = \Delta Q(p) - \frac{\Delta f_d}{(1 - f_d)}\underbrace{\frac{\beta_2}{\alpha_2}[\ln(\frac{1}{1-p})]^{1/\alpha_2 - 1}}_{\text{distorting term}} \tag{14}$$

This equation shows that the quantile trends in all-days can differ from the wet-days trends due to the change of rainfall occurrence, which acts as a weight in front of a distorting term (underlined by a curly brace in equation Equation (14)). Note that the distorting term is growing with p and its form changes with the shape parameter α, giving even larger additive trends for the heavy rain percentiles as α is small. Note that in the limit case where $\alpha \to 1$, this distorting term becomes a shift of constant value β_2: it is not anymore distorting the wet-days trend curve.

5.3 Modified regimes for all-days quantile trends

On historical data, it is important to quantify when and where the change of occurrence is large enough, compared to the wet-days quantile trends, to create relevant changes on the all-days quantile curves. We also want to analyze which percentiles will see their all-days trends the most impacted by Δf_d. We thus need to compare the Δf_d term to the $\Delta Q(p)$ term, in Equation (13).

The all-days trend is given by the wet-days trend if and only if, $\Delta Q_a(p_a) \approx \Delta Q(p)$ i.e. $|\Delta Q(p)| \gg \left|\frac{\Delta f_d}{1-f_d}\frac{\beta_2}{\alpha_2}\left[\ln\left(\frac{1}{1-p}\right)\right]^{1/\alpha_2-1}\right|$ At the first order, it is true if and only if :

$$\left|\frac{\partial Q}{\partial \alpha}(p)\Delta\alpha + \frac{\partial Q}{\partial \beta}(p)\Delta\beta\right| \gg \left|\frac{\Delta f_d}{1-f_d}\frac{\beta_2}{\alpha_2}\left[\ln\left(\frac{1}{1-p}\right)\right]^{1/\alpha_2-1}\right|$$

Let's look whether at least one of the two left-hand side terms is dominant over the term in Δf_d. The term due to the change of the scale parameter of the wet-days distribution dominates over the change of occurrence term for percentiles p such as:

$$\left|\ln\left(\frac{1}{1-p}\right)\right| \gg \left|\frac{\Delta f_d}{1-f_d}\frac{\beta_2}{\Delta\beta}\frac{1}{\alpha_2}\right|. \tag{15}$$

This is verified at least for ranks approaching 1 since $\lim_{p\to 1}\ln\left(\frac{1}{1-p}\right) = +\infty$. This independence of the maximum rainfall event trend from the rainfall occurrence was to be expected from Equation (10): $p = 1$ and $p_a = 1$ both describe the same event in wet-days and all-days. In addition, since the function $p \to \ln\left(\frac{1}{1-p}\right)$ is strictly growing on $[0, 1]$ up to infinity, there exists a percentile $p_{\lim,\Delta\beta}$ above which the function becomes larger than $|\frac{\Delta f_d}{1-f_d}\frac{\beta_2}{\Delta\beta}|\frac{1}{\alpha_2}$. Thus, quantiles of ranks between $p_{\lim,\Delta\beta}$ and $p = 1$ (the maximum rain event) will not be impacted by the change of dry-days.

As for the term due to the change of the shape of the wet-days distribution, it is dominant over the change of occurrence term only for percentiles p such as:

$$\left|\ln\left(\frac{1}{1-p}\right)\ln\left(\ln\frac{1}{1-p}\right)\right| \gg \left|\frac{\Delta f_d}{1-f_d}\frac{\alpha_2}{\Delta\alpha}\right|. \tag{16}$$

The left-hand side function is strictly growing on $[1-e^{-1}, 1]$ and tends to infinity at 1, thus there also exist a percentile rank $p_{\lim,\Delta\alpha}$ above which the function becomes larger than $|\frac{\Delta f_d}{1-f_d}\frac{\alpha_2}{\Delta\alpha}|$.

These two limit percentiles, $p_{\lim,\Delta\alpha}$ and $p_{\lim,\Delta\beta}$, can be inverted either analytically or numerically (using the classic segment or tangent methods). The maps of the factors $|\frac{\Delta f_d}{1-f_d}\frac{\beta_2}{\Delta\beta}\frac{1}{\alpha_2}|$ and $|\frac{\Delta f_d}{1-f_d}\frac{\alpha_2}{\Delta\alpha}|$ for ERA5 rain data are shown on the left column of Figure 5, followed by an illustration of the graphical inversion. The resulting maps for the limit percentiles are given at the bottom of the figure.

The figures show that $p_{\lim,\Delta\beta}$ is close to 100% for the Mediterranean, but much lower for most of Central and North Europe: its median on North-Central Europe (NCE) and West Central Europe (WCE) is respectively 46% and 40%. Thus, NCE and WCE, the terms depending on the change of dry-days frequency can be neglected compared to the change of wet-days scale parameter for wet-days percentiles larger than $p_{\lim,\Delta\beta} \approx 50\%$ (Figure 5).

We see that the percentile $p_{\lim,\Delta\alpha}$ is very high in Europe and the Mediterranean, usually above 90%, which signifies that the term in $\Delta\alpha$ is almost never dominant compared to the one in Δf_d for the all-days trend $\Delta Q_a(p_a)$. It means that in the Mediterranean, for the great majority of percentile ranks, their all-days trends are mainly due to the decrease of wet-days and not to a change of intensity when it rains. This is consistent with the low statistical significance of $\Delta\alpha$ over the domain on ERA5 data.

In summary, in most of the Mediterranean the all-days quantile trend curves will be largely impacted by the increase of dry-days frequency, leading to mostly "U-shape" and "all-decrease" categories. For most of Northern Europe in opposition, all-days quantile trend curves will be very similar to the wet-days', as the influence of $\Delta\beta$ is dominant in this region over the change of dry-days.

Figure 6 illustrates what the four wet-days categories trend can become in all-days trends, when the change of occurrence is not negligible.

In regions where the rainfall occurrence increases strongly enough, some locations with U-shape wet-days regime will become "all-increase" all-days regime (provided that the Δf_d term is large enough),

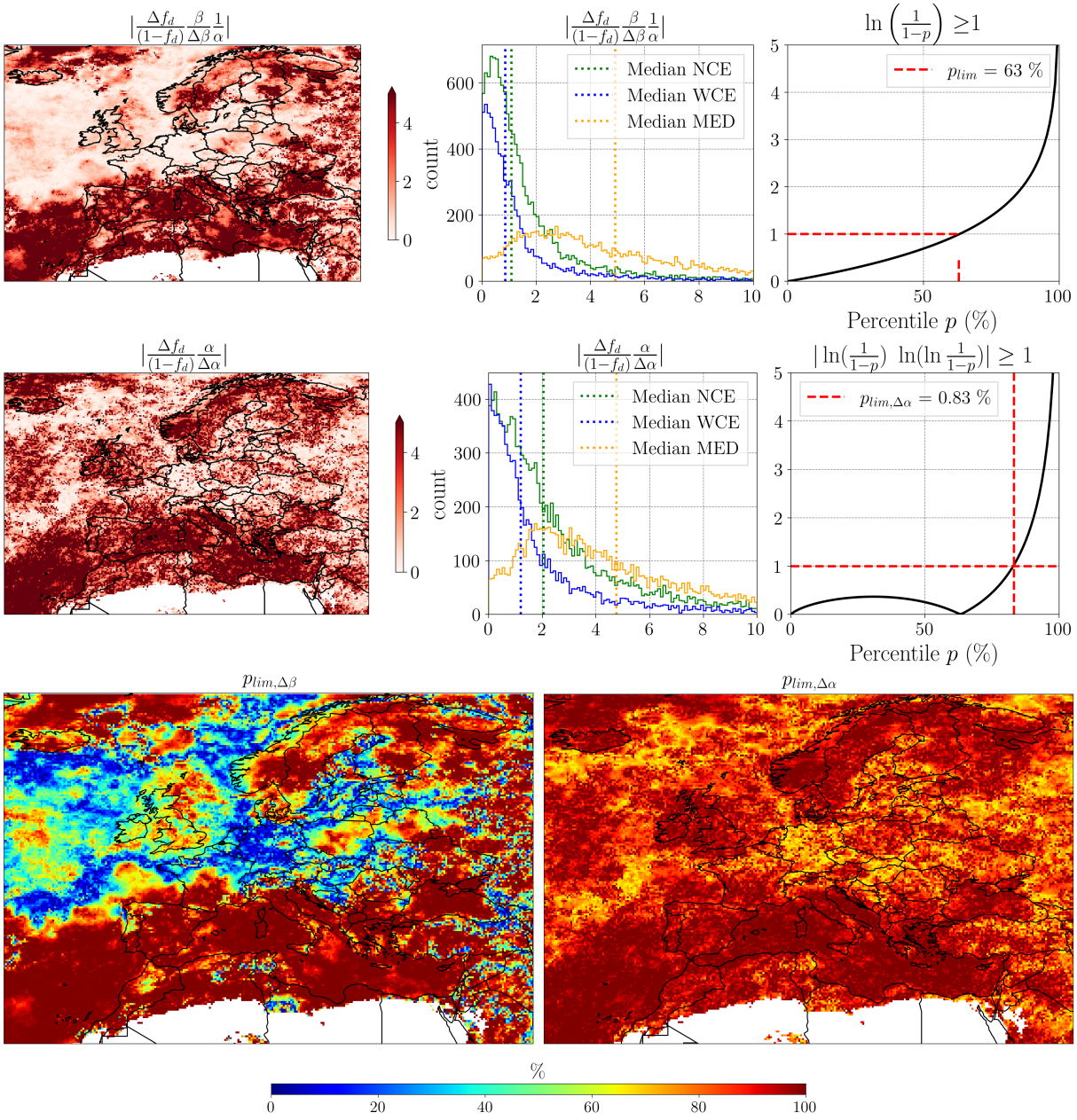

Figure 5: Left, top and middle figure: maps of the two factors determining the relative weight of the change of wet-days terms compared to the change of occurrence term for all-days trends. Middle top and middle figures: their histograms for the three IPCC regions (NCE = North Central Europe, WCE = West Central Europe, MED = Mediterranean). Right, top and middle figures: an example of the graphical inversion to find the limit percentile for the NCE median value. Bottom row: resulting maps for the limit percentiles $p_{\mathrm{lim},\Delta\alpha}$ and $p_{\mathrm{lim},\Delta\beta}$ (same color-bar). Like before, Δ denotes the changes between 1950–1980 and 1990–2020.

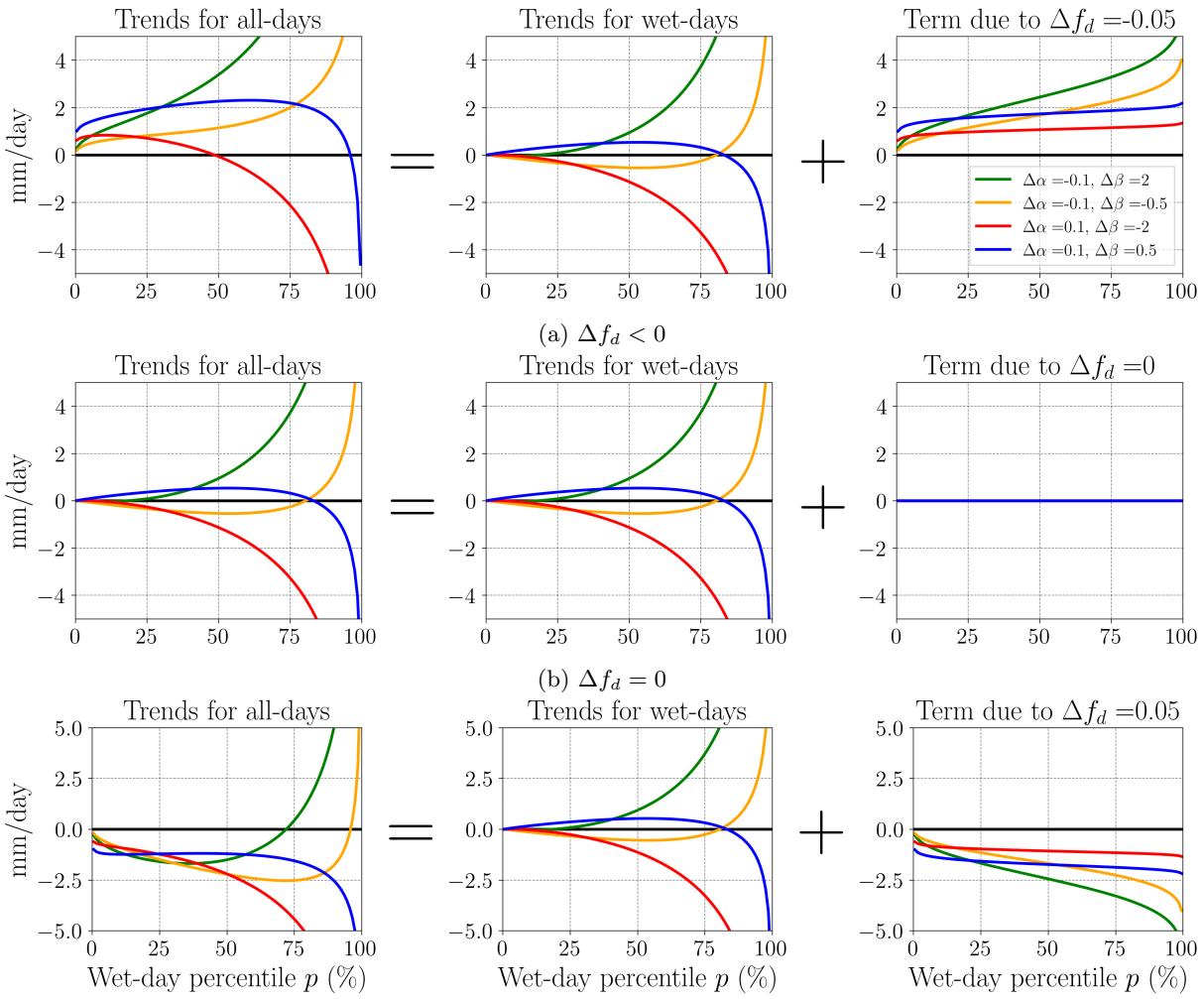

Figure 6: Illustration of the influence of the dry-days frequency term on the all-days quantile trend curves, for the four categories, for different values of the dry-days frequency change Δf_d. The values of the wet-days Weibull parameters ($\alpha, \beta, \Delta\alpha$ and $\Delta\beta$) are the same for all the subplots and are given on the top row. These values are synthetic.

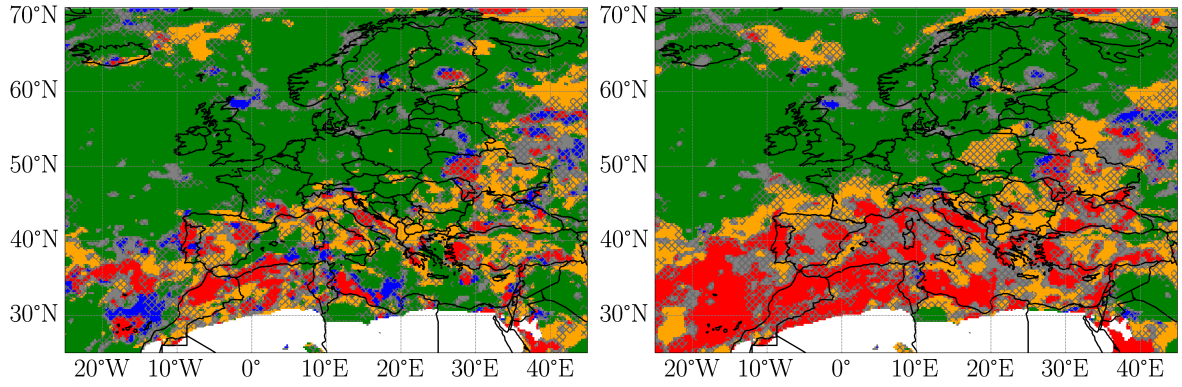

(a) Wet-days category map

(b) All-days category map

Figure 7: Category maps for the 1950–1980 and 1990–2020 periods. As before, green corresponds to "all quantiles intensify" category, red to "all quantiles decrease", orange to "U-shape" and blue to "reverse U-shape", while points whose category was unclear are in gray. White designates desert location (less than 2% of wet-days). The gray hatches denote places where the category detection is not very robust with regard to changes in the periods considered (cf Section 7.1).

while the wet-days "all-increase" trends will be more intense in all-days. Similarly, wet-days all-decrease will merge with inverse U-shape to give a new all-days "inverse U-shape". Thus, only two main regimes could exist for such regions in all-days distribution: "all-increase" and "reverse U-shape".

In regions where the rainfall occurrence decreases strongly, like in the Mediterranean, the opposite occurs: the "all-increase" wet-days regime will disappear in favor of an all-days "U-shape" regime, while wet-days U-shape's inversion percentile will become even larger in all-days. Similarly, the "reverse U-shape" will merge with the "all-decrease" category. Thus in all-days only, in regions with a strong decrease of f_d, only two regimes would be expected, "U-shape" and "all-decrease".

Figure 7 shows the resulting all-days categories, defined as explained in Section 7.1. It is put side by side with the wet-days categories map, to highlight the differences which are due to the change of dry-days frequency.

Note that gray hatches show the non robustness with the choice of the time period (cf Section 7.1). We see that both the wet-days and all-days category map are very robust over the northern part of Europe, while in the Mediterranean, most places' categories are not as robust, especially when at the frontier between different categories. Overall, the North-South pattern of all-days and wet-days categories is robust to the time periods considered.

In terms of spatial pattern, the overall North-South pattern of all-days category map is quite similar to the wet-days category map (Figure 1). We see that the all-days categories are generally smoother than the wet-days trends: there is a more continuous transition in latitude, with "all increase" in the North, "all decrease" in the South, and "U-shape" in between. Besides, the so called Mediterranean paradox, i.e. "U-shape" regime in all-days, is found in a transitional zone between wetting and drying, along Southern continental Europe, as well as in the Eastern part of the Mediterranean basin, but not the whole region as it was in wet-days. This is consistent with the fact that in the Mediterranean, the signal has been dominated by the increase of dry days, instead of the distortion of the wet-days distribution.

6 Conclusion

Climate change is known to impact greatly the Mediterranean region, which overall becomes warmer and drier, while the effects on extreme precipitations is still quite debated on historical data (Ali et al., 2022). In this study we aimed at better understanding how the strong trends of drying of the Mediterranean can influence the distribution of rain, all-together with the change of the whole wet-days distribution itself (from the low and medium percentiles to the most extreme rainfalls).

Using the ERA5 reanalysis, we studied the evolution of the wet-days rain distribution in the recent past, since the 1950s. We showed that it could evolve in four different regimes, defined on the quantiles trends curves: "all rain quantiles intensify", "all rain quantiles decrease", "U-shape" and "reversed U-shape". The map of the four regimes computed over Europe and the Mediterranean shows a strong

contrast between these two regions. While in Northern Europe all quantiles are intensifying with a clear and robust signal, the Mediterranean's regimes are shared between a dominant "U-shape" regime mixed with "all quantiles decrease", but are overall more spotty due to strong natural variability. This suggests that a climate change signal and its impact on the wet-days precipitation distribution, shift or distortion, have not (or not yet) emerged in the Mediterranean region, contrary to Northern Europe.

As for the map of regimes for the all-days distribution, it shows a clearer signal with latitude, from the Mediterranean ("all decrease") with a smooth transition (through a "U-shape" regime) to Northern Europe ("all increase" regime). The greater spatial uniformity of the all-day regime map in the Mediterranean comes from the stronger and more robust signal of dry-days frequency change, which dominates the all-day distribution trends.

By modeling the wet-days distribution with a Weibull law, we were able to reduce the information of the quantile trends to just two parameters, a scale and shape parameters, and their changes (representative of the precipitation distribution shift and distortion respectively). The categorization in four regimes can be estimated directly from the ratio and signs of the relative changes of the two Weibull parameters, as can be done for the percentile of inversion, when it exists. A statistical significance test on the change of the Weibull parameters confirms that a signal has emerged in Europe, with a strong increase of the scale parameter, i.e a shift of the whole distribution to more intense rainfall, without distortion. In the Mediterranean, only a few small regions have significant change of scale or shape parameter, reinforcing the argument that a climate change signal on wet-days has not yet emerged from natural variability.

Coming back to the whole distribution (including dry-days), we quantified how much some all-days important variables, such as the trends of the annual mean or of quantiles, are influenced by both the change of wet-days distribution and of dry-days frequency (the latter significantly increases in the Mediterranean but decreases in Northern Europe). The two effects can add up (as for the all-days mean in most of Northern Europe) or counterbalance each other (as in Southern Italy or in Poland).

The resulting all-days category map shows a clearer signal in latitude than the wet-days one: there is mostly "all rain quantiles intensify" in Northern Europe, then a transition with "U-shape" in a thin band of Central Europe, and finally the"all rain quantiles decrease" regime in most of the Mediterranean. Note that the so called Mediterranean paradox, i.e. "U-shape" regime in all-days, is thus not present in most of Mediterranean region, while it was dominant over this region when only wet-days were considered.

One of the key findings of the paper is that the change of dry-days frequency is predominant for the all-days trends of most quantiles in the Mediterranean, while in Northern Europe its effect can be neglected compared to the strong increase of the Weibull scale parameter, for all quantiles with wet-days rank above about 50%.

In a nutshell, the framework developed in this study establishes a connection between changes in wet-days precipitation and a few critical parameters that capture the shift and distortion of the precipitation distribution, as well as changes in precipitation occurrence. It has the potential to be employed in different geographical regions and time spans. In an upcoming publication, we intend to apply this framework to the future climate projections for the 21st century, in order to have a stronger and more robust signal over the Mediterranean. It would also enable to detect the year of emergence of the signal. Another potential application of this framework is the study of the physical processes that cause the observed changes, both from large-scale and local effects.

7 Open Research Section

Data availability statement: the hourly precipitation variable in ERA5 reanalysis Hersbach et al. (2018) was downloaded from the Copernicus Climate Change Service (C3S) accessed in July 2022. It is freely available on C3S website. The results contain modified Copernicus Climate Change Service information 2020. Neither the European Commission nor ECMWF is responsible for any use that may be made of the Copernicus information or data it contains.

7.1 Acknowledgements

CJM gratefully acknowledge funding from the European Research Council (ERC) under the European Union's Horizon 2020 research and innovation program (Project CLUSTER, Grant Agreement No. 805041). The authors also thank Samuel Somot (Centre National de Recherches Météorologiques, Toulouse) and Juliette Blanchet (Institut des Géosciences de l'Environnement, Grenoble) for their fruitful discussions on the project.

References

Ali, E., Cramer, W., Carnicer, J., Georgopoulou, E., Hilmi, N., Cozannet, G. L., and Piero, L. (2022). Cross-chapter paper 4: Mediterranean region. *Climate Change 2022: Impacts, Adaptation and Vulnerability*, pages 2233–2272.

Allen, M. R. and Ingram, W. J. (2002). Constraints on future changes in climate and the hydrologic cycle. *Nature*, 419(6903):224–232.

Alpert, P., Ben-Gai, T., Baharad, A., Benjamini, Y., Yekutieli, D., Colacino, M., Diodato, L., Ramis, C., Homar, V., Romero, R., Michaelides, S., and Manes, A. (2002). The paradoxical increase of Mediterranean extreme daily rainfall in spite of decrease in total values. *Geophysical Research Letters*, 29(11):31–1–31–4.

Ben-Gai, T., Bitan, A., Manes, A., Alpert, P., and Rubin, S. (1998). Spatial and temporal changes in rainfall frequency distribution patterns in israel. *Theoretical and Applied Climatology*, 61:177–190.

Benestad, R. E., Parding, K. M., Erlandsen, H. B., and Mezghani, A. (2019). A simple equation to study changes in rainfall statistics. *Environmental Research Letters*, 14(8):084017.

Berthou, S., Kendon, E. J., Chan, S. C., Ban, N., Leutwyler, D., Schär, C., and Fosser, G. (2020). Pan-European climate at convection-permitting scale: A model intercomparison study. *Climate Dynamics*, 55(1):35–59.

Berthou, S., Rowell, D. P., Kendon, E. J., Roberts, M. J., Stratton, R. A., Crook, J. A., and Wilcox, C. (2019). Improved climatological precipitation characteristics over west africa at convection-permitting scales. *Climate Dynamics*, 53:1991–2011.

Boberg, F., Berg, P., Thejll, P., Gutowski, W. J., and Christensen, J. H. (2010). Improved confidence in climate change projections of precipitation further evaluated using daily statistics from ENSEMBLES models. *Climate Dynamics*, 35(7):1509–1520.

Brunetti, M. (2004). Changes in daily precipitation frequency and distribution in Italy over the last 120 years. *Journal of Geophysical Research*, 109(D5):D05102.

Brunetti, M., Buffoni, L., Maugeri, M., and Nanni, T. (2000). Precipitation intensity trends in northern Italy. *International Journal of Climatology*, 20(9):1017–1031.

Caloiero, T., Caloiero, P., and Frustaci, F. (2018). Long-term precipitation trend analysis in Europe and in the Mediterranean basin. *Water and Environment Journal*, 32(3):433–445.

Colin, J. (2011). *Etude Des Événements Précipitants Intenses En Méditerranée : Approche Par La Modélisation Climatique Régionale*. PhD thesis, Université de Toulouse, Université Toulouse III - Paul Sabatier.

Cornes, R., Schrier, G., Van den Besselaar, E., and Jones, P. (2018). An Ensemble Version of the E-OBS Temperature and Precipitation Data Sets. *Journal of Geophysical Research Atmospheres*, 123.

D'Agostino, R. and Lionello, P. (2020). The atmospheric moisture budget in the Mediterranean: Mechanisms for seasonal changes in the Last Glacial Maximum and future warming scenario. *Quaternary Science Reviews*, 241:106392.

Drobinski, P., Da Silva, N., Bastin, S., Mailler, S., Muller, C., Ahrens, B., Christensen, O. B., and Lionello, P. (2020). How warmer and drier will the Mediterranean region be at the end of the twenty-first century? *Regional Environmental Change*, 20(3):12.

Drobinski, P., Silva, N. D., Panthou, G., Bastin, S., Muller, C., Ahrens, B., Borga, M., Conte, D., Fosser, G., Giorgi, F., Güttler, I., Kotroni, V., Li, L., Morin, E., Önol, B., Quintana-Segui, P., Romera, R., and Torma, C. Z. (2018). Scaling precipitation extremes with temperature in the Mediterranean: Past climate assessment and projection in anthropogenic scenarios. *Climate Dynamics*, 51(3):21.

Fischer, E. M., Beyerle, U., and Knutti, R. (2013). Robust spatially aggregated projections of climate extremes. *Nature Climate Change*, 3(12):1033–1038.

Fischer, E. M. and Knutti, R. (2014). Detection of spatially aggregated changes in temperature and precipitation extremes. *Geophysical Research Letters*, 41(2):547–554.

Giorgi, F. (2006). Climate change hot-spots. *Geophysical research letters*, 33(8).

Giorgi, F., Coppola, E., Raffaele, F., Diro, G. T., Fuentes-Franco, R., Giuliani, G., Mamgain, A., Llopart, M. P., Mariotti, L., and Torma, C. (2014). Changes in extremes and hydroclimatic regimes in the crema ensemble projections. *Climatic Change*, 125:39–51.

Groisman, P. Y., Karl, T. R., Easterling, D. R., Knight, R. W., Jamason, P. F., Hennessy, K. J., Suppiah, R., Page, C. M., Wibig, J., Fortuniak, K., et al. (1999). Changes in the probability of heavy precipitation: important indicators of climatic change. *Weather and climate extremes: changes, variations and a perspective from the insurance industry*, pages 243–283.

Held, I. M. and Soden, B. J. (2006). Robust Responses of the Hydrological Cycle to Global Warming. *Journal of Climate*, 19(21):5686–5699.

Herrera, S., Cardoso, R. M., Soares, P. M., Espírito-Santo, F., Viterbo, P., and Gutiérrez, J. M. (2019). Iberia01: A new gridded dataset of daily precipitation and temperatures over Iberia. *Earth System Science Data*, page 10.

Hersbach, H., Bell, B., Berrisford, P., Biavati, G., Horányi, A., Muñoz Sabater, J., Nicolas, J., Peubey, C., Radu, R., Rozum, I., et al. (2018). Era5 hourly data on single levels from 1959 to present [dataset]. copernicus climate change service (c3s) climate data store (cds). 10.24381/cds.adbb2d47 (accessed on 05-jul-2022).

Hersbach, H., Bell, B., Berrisford, P., Hirahara, S., Horányi, A., Muñoz-Sabater, J., Nicolas, J., Peubey, C., Radu, R., Schepers, D., Simmons, A., Soci, C., Abdalla, S., Abellan, X., Balsamo, G., Bechtold, P., Biavati, G., Bidlot, J., Bonavita, M., Chiara, G., Dahlgren, P., Dee, D., Diamantakis, M., Dragani, R., Flemming, J., Forbes, R., Fuentes, M., Geer, A., Haimberger, L., Healy, S., Hogan, R. J., Hólm, E., Janisková, M., Keeley, S., Laloyaux, P., Lopez, P., Lupu, C., Radnoti, G., Rosnay, P., Rozum, I., Vamborg, F., Villaume, S., and Thépaut, J.-N. (2020). The ERA5 global reanalysis. *Quarterly Journal of the Royal Meteorological Society*, 146(730).

Hoerling, M., Eischeid, J., Perlwitz, J., Quan, X., Zhang, T., and Pegion, P. (2012). On the Increased Frequency of Mediterranean Drought. *Journal of Climate*, 25(6):2146–2161.

Intergovernmental Panel On Climate Change (2023). *Climate Change 2021 – The Physical Science Basis: Working Group I Contribution to the Sixth Assessment Report of the Intergovernmental Panel on Climate Change*. Cambridge University Press, 1 edition.

Karl, T. R., Nicholls, N., and Ghazi, A. (1999). Clivar/gcos/wmo workshop on indices and indicators for climate extremes workshop summary. *Weather and climate extremes: Changes, variations and a perspective from the insurance industry*, pages 3–7.

Klingaman, N. P., Martin, G. M., and Moise, A. (2017). ASoP (v1.0): A set of methods for analyzing scales of precipitation in general circulation models. *Geoscientific Model Development*, 10(1):57–83.

Mariotti, A., Pan, Y., Zeng, N., and Alessandri, A. (2015). Long-term climate change in the Mediterranean region in the midst of decadal variability. *Climate Dynamics*, 44(5-6):20.

Myhre, G., Alterskjær, K., Stjern, C. W., Hodnebrog, Ø., Marelle, L., Samset, B. H., Sillmann, J., Schaller, N., Fischer, E., Schulz, M., and Stohl, A. (2019). Frequency of extreme precipitation increases extensively with event rareness under global warming. *Scientific Reports*, 9(1):16063.

Naveau, P., Huser, R., Ribereau, P., and Hannart, A. (2016). Modeling jointly low, moderate, and heavy rainfall intensities without a threshold selection. *Water Resources Research*, 52(4):2753–2769.

Peña-Angulo, D., Vicente-Serrano, S. M., Domínguez-Castro, F., Murphy, C., Reig, F., Tramblay, Y., Trigo, R. M., Luna, M. Y., Turco, M., Noguera, I., Aznárez-Balta, M., García-Herrera, R., Tomas-Burguera, M., and Kenawy, A. E. (2020). Long-term precipitation in Southwestern Europe reveals no clear trend attributable to anthropogenic forcing. *Environmental Research Letters*, 15(9):094070.

Pendergrass, A. G. and Hartmann, D. L. (2014). The atmospheric energy constraint on global-mean precipitation change. *Journal of climate*, 27(2):757–768.

Pfahl, S., O'Gorman, P. A., and Fischer, E. M. (2017). Understanding the regional pattern of projected future changes in extreme precipitation. *Nature Climate Change*, 7(6):423–427.

Pichelli, E., Coppola, E., Sobolowski, S., Ban, N., Giorgi, F., Stocchi, P., Alias, A., Belušić, D., Berthou, S., Caillaud, C., Cardoso, R. M., Chan, S., Christensen, O. B., Dobler, A., de Vries, H., Goergen, K., Kendon, E. J., Keuler, K., Lenderink, G., Lorenz, T., Mishra, A. N., Panitz, H.-J., Schär, C., Soares, P. M. M., Truhetz, H., and Vergara-Temprado, J. (2021). The first multi-model ensemble of regional climate simulations at kilometer-scale resolution part 2: Historical and future simulations of precipitation. *Climate Dynamics*, 56(11):3581–3602.

Pierce, D. W., Cayan, D. R., Das, T., Maurer, E. P., Miller, N. L., Bao, Y., Kanamitsu, M., Yoshimura, K., Snyder, M. A., Sloan, L. C., Franco, G., and Tyree, M. (2013). The Key Role of Heavy Precipitation Events in Climate Model Disagreements of Future Annual Precipitation Changes in California. *Journal of Climate*, 26.

Polade, S. D., Pierce, D. W., Cayan, D. R., Gershunov, A., and Dettinger, M. D. (2014). The key role of dry days in changing regional climate and precipitation regimes. *Scientific Reports*, 4(1):4364.

Raymond, F., Ullmann, A., Camberlin, P., Drobinski, P., and Smith, C. C. (2016). Extreme dry spell detection and climatology over the Mediterranean Basin during the wet season. *Geophysical Research Letters*, 43(13):9.

Rivoire, P., Le Gall, P., Favre, A.-C., Naveau, P., and Martius, O. (2022). High return level estimates of daily era-5 precipitation in europe estimated using regionalized extreme value distributions. *Weather and climate extremes*, 38:100500.

Rivoire, P., Martius, O., and Naveau, P. (2021). A Comparison of Moderate and Extreme ERA-5 Daily Precipitation With Two Observational Data Sets. *Earth and Space Science*, 8(4):e2020EA001633.

Schär, C., Ban, N., Fischer, E. M., Rajczak, J., Schmidli, J., Frei, C., Giorgi, F., Karl, T. R., Kendon, E. J., Tank, A. M. G. K., O'Gorman, P. A., Sillmann, J., Zhang, X., and Zwiers, F. W. (2016). Percentile indices for assessing changes in heavy precipitation events. *Climatic Change*, 137(1):201–216.

Sheffield, J. and Wood, E. F. (2012). *Drought: Past Problems and Future Scenarios*. Routledge.

Sousa, P. M., Trigo, R. M., Aizpurua, P., Nieto, R., Gimeno, L., and García Herrera, R. (2011). Trends and extremes of drought indices throughout the 20th century in the Mediterranean. *Natural hazards and earth system sciences*, 11(1):19.

Tanarhte, M., Hadjinicolaou, P., and Lelieveld, J. (2012). Intercomparison of temperature and precipitation data sets based on observations in the mediterranean and the middle east. *Journal of Geophysical Research: Atmospheres*, 117(D12).

Tencaliec, P., Favre, A.-C., Naveau, P., Prieur, C., and Nicolet, G. (2020). Flexible semiparametric generalized pareto modeling of the entire range of rainfall amount. *Environmetrics*, 31(2):e2582.

Trenberth, K. E. (1999). Conceptual Framework for Changes of Extremes of the Hydrological Cycle with Climate Change. *Climatic Change*, 42(1):327–339.

Trenberth, K. E. (2011). Changes in precipitation with climate change. *Climate Research*, 47(1-2):123–138.

Vautard, R., Gobiet, A., Sobolowski, S., Kjellström, E., Stegehuis, A., Watkiss, P., Mendlik, T., Landgren, O., Nikulin, G., Teichmann, C., and Jacob, D. (2014). The european climate under a 2 °C global warming. *Environmental Research Letters*, 9(3):12.

Zhang, X., Alexander, L., Hegerl, G. C., Jones, P., Tank, A. K., Peterson, T. C., Trewin, B., and Zwiers, F. W. (2011). Indices for monitoring changes in extremes based on daily temperature and precipitation data. *WIREs Climate Change*, 2(6):851–870.

Zittis, G. (2018). Observed rainfall trends and precipitation uncertainty in the vicinity of the Mediterranean, Middle East and North Africa. *Theoretical and Applied Climatology*, 134(3):1207–1230.

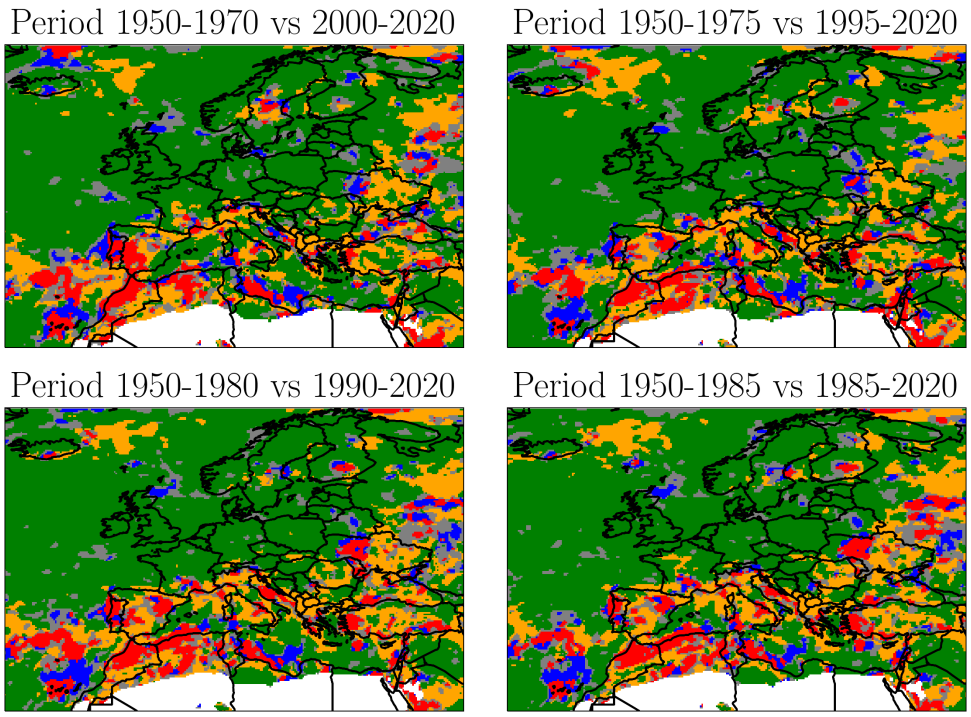

Figure 8: Category maps for wet-days quantile trends computed for different couples of time periods over 1950-2020. The quantile trends values leading to this map have been processed by a smoothing window of 9 points. As before, green color corresponds to "all quantiles intensify" category, red to "all quantiles decrease", orange to "U-shape" and blue to "reverse U-shape".

Appendix A: Influence of the time period

In Figure 8, we can see the wet-days category maps computed for different time periods, covering the 1950–2020 periods:

- 1950-1970 vs 2000-2020
- 1950-1975 vs 1995-2020
- 1950-1980 vs 1990-2020
- 1950-1985 vs 1985-2020

At a given location, the category of the reference period is considered as robust if at least 3 or the 4 pairs of periods give the same category. This criterion is used to define both for wet-days and all-days category's robustness, which is represented by the gray hatches on Figure 7.

Appendix B: Algorithm for detection of regimes

In order to quantitatively distinguish between the different regimes of trends, we developed a classification algorithm, which takes in a list of percentiles and the associated quantile trends (previously computed between two times periods), looks at the shape of the trend curve and assesses in which of the four categories it falls into.

For wet-days percentiles, we define the belly of the curve as the part of the curve between the 10th and the 60th percentiles, and the tail as the part of the curve between the 85th and the 99th quantiles. We also define the slope of the tail as the slope of the linear regression of the curve between the 60th and the 99th quantiles. The algorithm is the following:

1. If the means of both the belly and the tail are positive and that the slope of the tail is positive, then the category is defined as "all quantiles intensify".

2. If the mean of the belly is negative, but the tail has a positive mean and slope, then the category is defined as "U-shape".

3. If the mean of the belly is negative and the tail has a negative mean and slope, then the category is defined as "all quantiles decrease".

4. If the mean of the belly is positive while the tail has a negative mean and a negative slope, then the category is defined as "reversed U-shape".

Finally, if the curve doesn't fall into any of these four categories, it is set into the "unknown" category.

For all-days category, the definition is slightly different. It consists in computing the all-days quantile trends (from percentiles $p_a \in [0, 1]$) and then applying the above algorithm only on the equivalent wet-days percentiles p_w, corresponding to $p_a \in [f_d, 1]$. For this, we have chosen to use the value of dry-days frequency f_d of the reference period (1950–1980).

Appendix C: Comparison of distribution models for ERA5 rainfall

There is no *a priory* clear choice for a parametric model for the whole wet-days distribution of daily rain (rain above threshold, here 1 mm/day). The choice of a particular model may depend a lot on the region considered, on the origin of the data (station data, spatial interpolation from stations, satellite data, reanalysis, or climate projections), on its spatial and temporal resolution, ... We have therefore tested on ERA5 daily rain data, a list of the most common models (as well as the distribution from (Naveau et al., 2016), called Naveau in the following). To compare the quality of the different models, we used two goodness of fit estimators, computed on cumulative density functions: Kolmogorov-Smirnov (a L1 distance) and Cramer von Mises (a L2 distance). When a location parameter was needed, we set it at the wet-days threshold (1 mm/day).

We found that in average, the best distribution for the Mediterranean region was the Naveau law, followed by the Weibull law and the Gamma law (Figure 9). As the Naveau model has more complexity (three parameters) than what we need to capture the quantile trends regimes, we decided not to select this model. We compared Weibull and Gamma laws pixel-wise across the whole Europe and Mediterranean. The ratio of the fitting error of Weibull vs. Gamma laws shows that the Weibull model is more suitable than Gamma law, in most of the Mediterranean domain. We therefore choose the Weibull law for our model.

Once we fitted the Weibull law on a time serie and that we got its optimal fit parameters, we used the usual Kolmogorov-Smirnov distance as an adjustment test: if this distance is "small enough", the fit is accepted. According to empirical tables, for a confidence level of 95%, the Kolmogorov-Smirnov distance is considered small enough if falling below $1.36/\sqrt{N}$, where N is the number of data points, as far as $N > 35$ (which is largely the case since we fit Weibull on daily data on several decades). The mask of where the Weibull fit doesn't pass the adjustment test is shown by hatches on Figure 9. It shows that Weibull is indeed an acceptable model for most of the domain (except for some Mediterranean coastal areas and sea area in the Atlantic west of Portugal).

Appendix D: Statistical significance test

We are interested in their statistical significance of different statistics computed on the data, such as the quantile trends or the Weibull parameters trends. As the rainfall data on the Mediterranean region is spatially and temporally correlated, we perform a bootstrap test. It consists in comparing the trend of the real data with the trends that would be obtained on a large number (typically a hundred) of artificial samples presenting a spatial and temporal variability similar to our original data. Each sample is an artificial time serie created by pulling random days from our 1950–2020 original data (with replacement). The artificial time series have the same length as the original one.

Since the dates have been mixed in the artificial samples, their average linear trends are zero, but their variability gives us an estimation of the noise in our original data. The trend of the original data is said significant at a given level, for example 90%, if the original data lies within the 10% more extreme

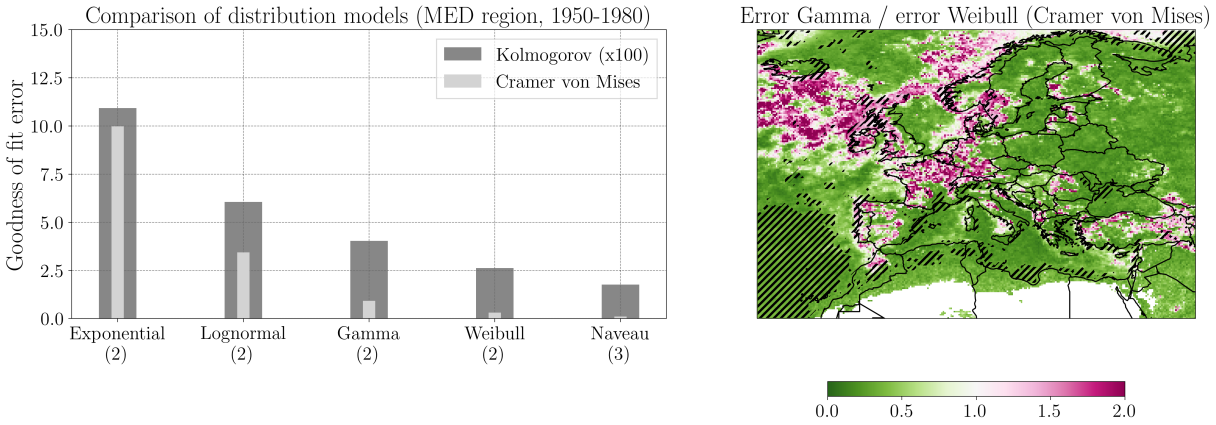

Figure 9: Left: goodness of fit estimator for different wet-days distribution models on the Mediterranean region (as defined by the IPCC) with a smoothing window of 9 points. Note that we used a scale factor for the Kolmogorov–Smirnov estimator, which was much smaller than Cramer von Mises estimator. In the x-axis, the number in parentheses is the number of parameters of the fit. Right: Map of the ratio of errors (Cramer von Mises goodness of fit) between Gamma and models, across the whole domain. In green are all the location where Weibull model is better suited for the data than Gamma. Black hatches show the locations where the adjustment test of the Weibull model fails, with a confidence level of 95%.

values of the bootstrap distribution, meaning that we could have the original data "by chance" from this random distribution only with low probability (less than 10%).

Appendix E: Inversion percentile

When the regime is a "U-shape", the quantile curve has negative trends up to a certain percentile rank, which we will define as the "inversion percentile". After that rank, almost all the following percentiles have positive trends. We can get an analytical expression for the inversion percentile p_{inv} with the Weibull model, by solving the equations $\Delta Q(p_{inv}) = 0$ for $p_{inv} > 0$. This results in the following expression:

$$p_{inv} = 1 - \exp\left(-\left(\frac{\beta_2}{\beta_1}\right)^{\frac{\alpha_1\alpha_2}{\alpha_2-\alpha_1}}\right) \tag{17}$$

Since the changes of α and β are small for rainfall in ERA5 data (about a few percents), we can simplify this expression. Let's write $\Delta\alpha = \alpha_2 - \alpha_1$ and $\alpha = (\alpha_2 + \alpha_1)/2$, and similarly for β, then we have $\frac{\beta_2}{\beta_1} \approx 1 + \frac{\Delta\beta}{\beta}$ and $\frac{\alpha_1\alpha_2}{\alpha_2-\alpha_1} \approx \frac{\alpha^2}{\Delta\alpha}$, and we can simplify the exponent:

$$\ln\left(\frac{\beta_2}{\beta_1}^{\frac{\alpha_1\alpha_2}{\alpha_2-\alpha_1}}\right) = \frac{\alpha_1\alpha_2}{\alpha_2-\alpha_1}\ln\left(\frac{\beta_2}{\beta_1}\right) \approx \frac{\alpha^2}{\Delta\alpha}\ln\left(1+\frac{\Delta\beta}{\beta}\right) \approx \frac{\alpha^2}{\Delta\alpha}\frac{\Delta\beta}{\beta}$$

where the last approximation is done by taking the development at the first order in $\Delta\beta/\beta$. We finally get this expression for the inversion percentile:

$$p_{inv} \approx 1 - \exp\left(-\exp(\frac{\Delta\beta}{\beta}\frac{\alpha^2}{\Delta\alpha})\right) \tag{18}$$

Geometrically speaking, this means that at first approximation, the angle in the Weibull parameter space $(X, Y) = \left(\frac{\Delta\beta}{\beta}, \frac{\Delta\alpha}{\alpha^2}\right)$ gives the value for the inversion percentile p_{inv}.

We can also derive a lower and upper limit for the inversion percentile. Indeed, the inversion percentile is properly defined only in the case where the change of α dominates (U-shape or reversed U-shape), i.e. when $\left|\frac{\Delta\alpha}{\alpha^2}\frac{\beta}{\Delta\beta}\right| \gg 1$. The limit cases for this to be true would be when the change in α doesn't dominate anymore, i.e. when $\frac{\Delta\alpha}{\alpha^2}\frac{\beta}{\Delta\beta}$ is close to -1 or 1. Those two cases give the minimal and maximal values of p_{inv} for a U-shape according to the Weibull law are: $p_{0,\min} \approx 1 - e^{-e^{-1}} \approx 30\%$ and $p_{0,\max} \approx 1 - e^{-e^{1}} \approx 93\%$. These values are consistent with the range of inversion percentile observed on the reanalysis (not shown).